Magn Reson Med Sci 2023; 22; 87–94
doi:10.2463/mrms.mp.2021-0015
Published Online: March 10, 2022

MAJOR PAPER

Efficacy of Quantitative Susceptibility Mapping with Brain Surface Correction and Vein Removal for Detecting Increase Magnetic Susceptibility in Patients with Alzheimer's Disease

Akinori Yamaguchi[1], Kohsuke Kudo[1,2*], Ryota Sato[3], Yasuo Kawata[3], Niki Udo[4], Masaaki Matsushima[5], Ichiro Yabe[5], Makoto Sasaki[6], Masafumi Harada[7], Noriyuki Matsukawa[8], Toru Shirai[3], Hisaaki Ochi[3], and Yoshitaka Bito[3]

Purpose: Studies on quantitative susceptibility mapping (QSM) have reported an increase in magnetic susceptibilities in patients with Alzheimer's disease (AD). Despite the pathological importance of the brain surface areas, they are sometimes excluded in QSM analysis. This study aimed to reveal the efficacy of QSM analysis with brain surface correction (BSC) and/or vein removal (VR) procedures.

Methods: Thirty-seven AD patients and 37 age- and sex-matched, cognitively normal (CN) subjects were included. A 3D-gradient echo sequence at 3T MRI was used to obtain QSM. QSM images were created with regularization enabled sophisticated harmonic artifact reduction for phase data (RESHARP) and constrained RESHARP with BSC and/or VR. We conducted ROI analysis between AD patients and CN subjects who did or did not undergo BSC and/or VR using a t-test, to compare the susceptibility values after gray matter weighting.

Results: The susceptibility values in RESHARP without BSC were significantly larger in AD patients than in CN subjects in one region (precentral gyrus, 8.1 ± 2.9 vs. 6.5 ± 2.1 ppb) without VR and one region with VR (precentral gyrus, 7.5 ± 2.8 vs. 5.9 ± 2.0 ppb). Three regions in RESHARP with BSC had significantly larger susceptibilities without VR (precentral gyrus, 7.1 ± 2.0 vs. 5.9 ± 2.0 ppb; superior medial frontal gyrus, 5.7 ± 2.6 vs. 4.2 ± 3.1 ppb; putamen, 47,8 ± 16.5 vs. 40.0 ± 15.9 ppb). In contrast, six regions showed significantly larger susceptibilities with VR in AD patients than in CN subjects (precentral gyrus, 6.4 ± 1.9 vs. 4.9 ± 2.7 ppb; superior medial frontal gyrus, 5.3 ± 2.7 vs. 3.7 ± 3.3 ppb; orbitofrontal cortex, –2.1 ± 2.7 vs. –3.6 ± 3.2 ppb; parahippocampal gyrus, 0.1 ± 3.6 vs. –1.7 ± 3.7 ppb; putamen, 45.0 ± 14.9 vs. 37.6 ± 14.6 ppb; inferior temporal gyrus, –3.4 ± 1.5 vs. –4.4 ± 1.5 ppb).

Conclusion: RESHARP with BSC and VR showed more regions of increased susceptibility in AD patients than in CN subjects. This study highlights the efficacy of this method in facilitating the diagnosis of AD.

Keywords: *Alzheimer's disease, brain surface correction, cerebral cortex, quantitative susceptibility mapping, vein removal*

[1]Department of Diagnostic Imaging, Hokkaido University Graduate School of Medicine, Sapporo, Hokkaido, Japan
[2]Global Center for Biomedical Science and Engineering, Faculty of Medicine, Hokkaido University, Sapporo, Hokkaido, Japan
[3]FUJIFILM Healthcare Corporation, Tokyo, Japan
[4]Department of Psychiatry, Hokkaido University Graduate School of Medicine, Sapporo, Hokkaido, Japan
[5]Department of Neurology, Hokkaido University Graduate School of Medicine, Sapporo, Hokkaido, Japan
[6]Division of Ultrahigh Field MRI, Institute for Biomedical Sciences, Iwate Medical University, Morioka, Iwate, Japan
[7]Department of Radiology, Tokushima University Graduate School of Medicine, Tokushima, Tokushima, Japan
[8]Department of Neurology, Nagoya City University Graduate School of Medical Sciences, Nagoya, Aichi, Japan
*Corresponding author: Faculty of Medicine, Hokkaido University, Kita15, Nishi7, Kita-Ku, Sapporo, Hokkaido 060-8638, Japan. Phone: +81-11-706-7779, Fax: +81-11-706-7408, E-mail: kkudo@med.hokudai.ac.jp

Received: February 1, 2021 | Accepted: January 7, 2022

Introduction

Alzheimer's disease (AD) is a complex neurodegenerative disease characterized by cognitive decline and memory loss.[1,2] AD primarily affects the elderly, and the number of patients has been increasing with the aging society. Currently, a definitive diagnosis of AD can only be made postmortem, and *in vivo* biomarkers are lacking. This calls for the need to diagnose AD at an early age.

Two neuropathological features reported in the brain of patients with AD are as follows: (1) the deposit of senile plaques outside neurons with amyloid-beta (Aβ) accumulation and (2) the deposit of neurofibrillary tangles inside neurons with tau accumulation.[3] Positron emission tomography (PET) studies of amyloid and tau accumulation have established imaging biomarkers;[4,5] however, the PET scanners are not widely accessible, and the cost is too high.

MRI is available at most large hospitals. MRI-based diagnosis assesses atrophy in the medial temporal lobe by visual evaluation or voxel-based morphometry (VBM).[6] In addition, several studies have reported on the utility of quantitative susceptibility mapping (QSM). A study showed higher magnetic susceptibilities in the deep gray matter in AD patients.[7] Another study showed higher magnetic susceptibilities in the frontal and temporal cortex.[8] However, how magnetic susceptibilities in the cortex are shown by divided ROIs is poorly documented. This is possibly due to the coexistence of iron with amyloid plaques and tau tangles.[9] Furthermore, such patients are characterized by a disruption of iron homeostasis,[10] and iron deposition is related to the secondary cytopathic effect and ferroptosis.[11,12]

The deposition of amyloid and tau predominantly occurs in the neocortex; however, those areas are sometimes masked out during QSM reconstruction. Furthermore, the measurement of cortical susceptibilities becomes inaccurate because of the contamination of venous susceptibilities. The latter is usually higher than the cortex. This can be attributed to the presence of deoxy-hemoglobin. Therefore, we hypothesized that the measurement of cortical susceptibilities in AD patients is more accurate with brain surface correction (BSC) and vein removal (VR).

This study aimed to compare susceptibility values between AD patients and cognitively normal (CN) subjects who did or did not undergo BSC and/or VR procedures.

Materials and Methods

Subjects

This combined prospective and retrospective study was approved by the Ethical Review Board for Life Science and Medical Research, Hokkaido University Hospital (017–0073). We obtained written informed consent from the prospectively recruited subjects. The retrospectively included subjects were given the opportunity to opt-out from the study via the institutional website. We enrolled patients with cognitive decline from May 10, 2017 to May 15, 2019. The inclusion criteria were as follows: (a) diagnosed with AD by a neurologist or psychiatrist using the Diagnostic and Statistical Manual of Mental Disorders, Fifth Edition; (b) aged between 20 and 89 years at the time of informed consent; (c) with MRI scans conducted within a month after providing consent; (d) free will to participate and capable of comprehending the information conveyed; and (e) allowed proxy consent when the subjects could not consent adequately because of dementia. In contrast, the exclusion criteria were as follows: (a) those with contraindications for MRI, such as cardiac pacemaker and deep brain stimulation device; (b) confirmed or suspected pregnancy; (c) with claustrophobia; and (d) patients who were considered inappropriate for our study. We eventually considered 46 patients appropriate for this study.

We also included CN subjects with the following inclusion criteria: (a) aged between 20 and 89 years while providing informed consent; (b) with Mini-Mental State Examination (MMSE) score > 26[13] and the Japanese version of the Montreal Cognitive Assessment (MoCA-J) score > 25;[14] and (c) willingly agreed to participate and understood the information conveyed adequately. In contrast, the exclusion criteria were as follows: (a) those with central nervous system diseases and neuropsychiatric illnesses; (b) with contraindications, such as cardiac pacemakers and deep brain stimulation devices; (c) with claustrophobia; (d) confirmed or suspected pregnancy; and (e) those subjects who were considered inappropriate for the study. We eventually recruited 112 CN subjects for this study.

MRI

We performed MRI using a 3-T scanner (Hitachi, Tokyo, Japan). A 3D-gradient echo sequence was used to obtain QSM. The scan parameters included flip angle, 45°; TR, 38 ms; six TE of 4.3, 9.6, 14.9, 20.2, 25.5, and 30.8 ms; FOV, 240 mm; imaging matrix, 344 × 240; slice thickness, 2 mm; slab thickness, 200 mm; and parallel imaging factor, 1.7 × 1.9.

Data Analysis

We reconstructed the phase images of all echoes to generate a QSM image. Moreover, we segmented the magnitude image of the first echo to obtain an image of the gray matter. The QSM reconstruction process consisted of unwrapping of the region-growing phase, phase averaging with magnitude weighting, background field removal, and field-to-susceptibility inversion. Regularization enabled sophisticated harmonic artifact reduction for phase data (RESHARP) was the method for background field removal.[15] The radius of the spherical mean value (SMV) kernel size was 5 mm. The RESHARP method cannot be used to calculate the local field of the brain edge corresponding to the radius of the SMV convolution kernel. Thus, we used constrained RESHARP with BSC. It facilitated background field

calculation by local polynomial approximation.[16] The fitting range was 5 × 5 × 5 mm. This method enabled us to calculate a brain-surface local field and obtain susceptibility data, including brain surfaces.

We implemented the process of the field-to-susceptibility inversion by least-squares estimation with adaptive edge-preserving filtering (LSE with AEPF).[17] This method consists of the following three steps: (I) iterative least-square minimization, (II) adaptive and edge-preserving filtering to the susceptibility map in the minimization process, and (III) weighted addition of the susceptibility map in the k-space before and after filtering. This method allowed the reduction in the streaking artifacts and generated a high-quality quantitative susceptibility map without the regularization term (Fig. 1a).

We applied VR to the QSM images with the following steps: extracting venous voxels with morphology edge-enhanced filtering, followed by thresholding and replacing the venous voxels with an averaged value in a surrounding square kernel (Fig. 1b). The kernel size was set to 7 × 7 pixels to cover large subcortical veins. We spatially normalized the images obtained using the Diffeomorphic Anatomical Registration Through Exponentiated Lie Algebra (DARTEL) algorithm.[18] We applied gray matter segmentation to the 1st echo magnitude image (TE = 4.3 mm) and subsequently calculated the gray matter weighted susceptibility values.

Four types of data prepared for further analysis were as follows: RESHARP (with or without VR) and RESHARP with BSC (with or without VR). We performed the ROI analysis for each data with an automated anatomical labeling template for 120 regions.[19,20] We selected 94 regions, except the subtentorial areas that were not associated with the pathological features of AD. Following the averaging of the left and right regions, we evaluated 47 regions.

Statistical test

We compared the susceptibility values of each region between the AD and CN groups using a t-test and an open-source software for statistical analyses (R version 3.6.2 [2019-12-12]). We evaluated how MMSE scores were associated with the susceptibility values using a scatter plot. A P value < 0.05 was considered statistically significant.

Results

Of the 46 patients, we excluded nine patients because of strong motion artifacts (n = 5), unknown artifacts (n = 1), and microbleeds (n = 3). Thus, we included 37 patients with AD (20 men and 17 women) in this study. Similarly, we excluded four subjects of the 112 CN subjects because of metal artifact (n = 1), venous malformation (n = 1), calcification of the falx (n = 1), and cystic lesions in white matter (n = 1). Besides, we excluded 72 subjects below the age of 65 years and four women and included five men. Eventually, 37 age- and sex-matched CN subjects were included in this study. They comprised 20 men and 17 women. The mean ages of the AD patients and the CN subjects were 75.7 (range, 57–90) and 73.8 (range, 57–86) years, respectively. There was no significant difference in age between the AD patients and CN subjects (P = 0.34). The mean MMSE scores for the 28 AD patients and 37 CN subjects were 21.3 (range, 8–29) and 29.2 (range, 27–30), respectively.

The susceptibility values of AD in RESHARP were significantly larger than those of CN in one region (precentral gyrus, 8.1 ± 2.9 vs. 6.5 ± 2.1 ppb, P < 0.01) without VR (Fig. 2a), and one region (precentral gyrus, 7.5 ± 2.8 vs. 5.9 ± 2.0 ppb, P < 0.01) with VR (Fig. 2b). Three regions had significantly larger susceptibilities without VR (precentral gyrus, 7.1 ± 2.0 vs. 5.9 ± 2.0 ppb, P < 0.01; superior medial frontal gyrus, 5.7 ± 2.6 vs. 4.2 ± 3.1 ppb, P < 0.05; putamen, 47.8 ± 16.5 vs. 40.0 ± 15.9 ppb, P < 0.05) in RESHARP with BSC (Fig. 2c). In contrast, six regions showed significantly larger susceptibilities with VR in AD, compared to CN (precentral gyrus, 6.4 ± 1.9 vs. 4.9 ± 2.7 ppb, P < 0.01; superior medial frontal gyrus, 5.3 ± 2.7 vs. 3.7 ± 3.3 ppb, P < 0.05; orbitofrontal cortex, –2.1 ± 2.7 vs. –3.6 ± 3.2 ppb, P < 0.05; parahippocampal gyrus, 0.1 ± 3.6 vs. –1.7 ± 3.7 ppb, P < 0.05; putamen, 45.0 ± 14.9 vs. 37.6 ± 14.6 ppb, P < 0.05; inferior temporal gyrus, –3.4 ± 1.5 vs. –4.4 ± 1.5 ppb, P < 0.05) (Fig. 2d, Table 1).

MMSE score had significant correlation with the susceptibility values in two regions (precentral gyrus; $y = -0.14x + 9.12$, $R^2 = 0.08$, $P = 0.02$, superior medial frontal gyrus; $y = -0.16x + 8.66$, $R^2 = 0.07$, $P = 0.04$). In contrast, we could not find significant correlation in four regions (orbitofrontal cortex; $y = -0.13x + 0.54$, $R^2 = 0.04$, $P = 0.10$, parahippocampal gyrus; $y = -0.16x + 3.22$, $R^2 = 0.05$, $P = 0.09$, putamen; $y = -0.60x + 56.51$, $R^2 = 0.04$, $P = 0.13$, inferior temporal gyrus; $y = -0.04x - 2.74$, $R^2 = 0.02$, $P = 0.26$) (Fig. 3, Table 2).

Discussion

The novel method of BSC and VR revealed more regions of the cerebral cortex with significantly higher susceptibilities in AD patients than in CN subjects. The pathological features of AD include the deposition of Aβ and tau in the neocortex. Thus, the use of the aforementioned procedures in QSM successfully demonstrated an increased susceptibility in the cerebral cortex because of iron deposition in association with Aβ and tau or disrupted iron homeostasis. However, it should be noted that Aβ distribution imperfectly matches an increased susceptibility because of the secondary cytopathic effect and ferroptosis.

Increased susceptibility in the frontal and temporal cortex is compatible with AD pathology. However, we observed the areas of increased susceptibility in the precentral gyrus. AD pathology is not expected in those areas at an early stage. Aβ accumulation in the precentral gyrus reportedly occurs slowly. In addition, Aβ accumulation

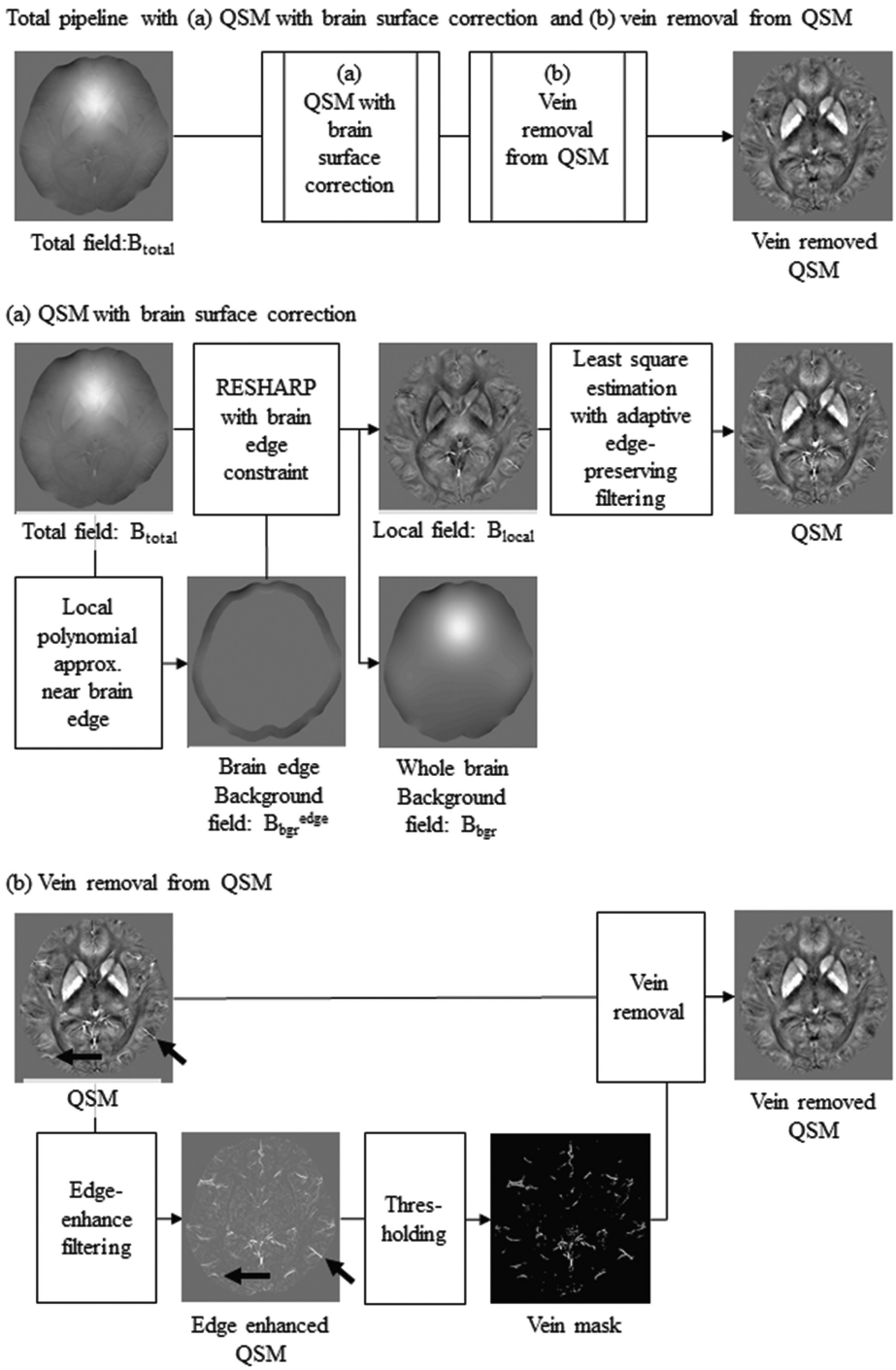

Fig. 1 Our proposing pipeline with (**a**) QSM with brain surface correction and (**b**) vein removal from QSM. (**a**) shows the process flow of QSM with brain surface correction. First, the background field of the brain edge is calculated from the total field using local polynomial approximation. Second, the local field of the whole brain is calculated by the RESHARP processing method with a constraint term of the background field of the brain edge R1. Finally, QSM is calculated by the least-square estimation with adaptive edge-preserving filtering (LSE-AEPF). (**b**) shows the process flow of vein removal for the QSM image. In the removal process, regions of veins (arrows) were enhanced by morphological edge-enhanced filtering and extracted by thresholding (0.03 ppb). Then, the veins were removed by replacing the vein regions with the averaged susceptibility value in a surrounding 7 × 7 pixel square kernel.

occurs in the precuneus/posterior cingulate, frontal cortex, and caudate nucleus, followed by the lateral temporal and parietal cortex in AD patients.[21] We did not observe any substantial increase in susceptibility in the precuneus/posterior cingulate ($P = 0.41/0.99$ in RESHARP with BSC and VR) and caudate nucleus ($P = 0.15$ in RESHARP with BSC

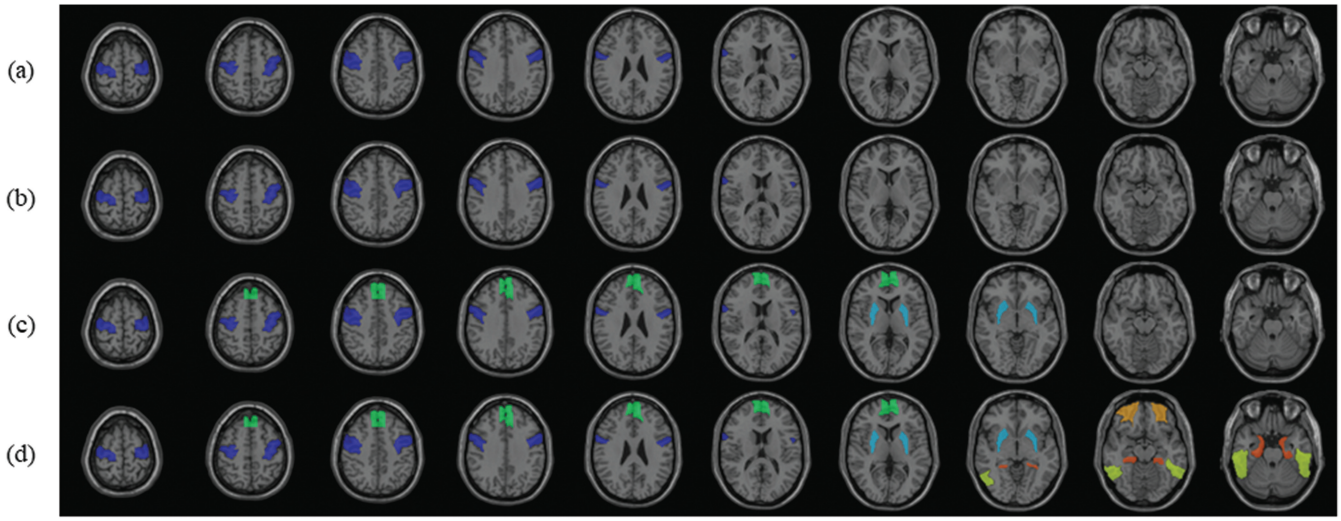

Fig. 2 Areas of increased susceptibility in AD patients compared to CN subjects, displayed on T1-weighted images. (**a**) RESHARP (without VR): Significant increase in the susceptibility in AD patients compared to those in CN subjects in one region, namely, the precentral gyrus (dark blue). (**b**) RESHARP (with VR): Significant increases in the susceptibility in AD patients compared to those in CN subjects in one region, namely, the precentral gyrus (dark blue). (**c**) RESHARP with BSC (without VR): Three regions showed significant increases in the susceptibility in AD patients, namely, the precentral gyrus (dark blue), superior medial frontal gyrus (green), and putamen (light blue). (**d**) RESHARP with BSC (with VR): Six regions showed significant increases in the susceptibility in AD patients, including the precentral gyrus (dark blue), superior medial frontal gyrus (green), orbitofrontal cortex (orange), parahippocampal gyrus (red), putamen (light blue), and inferior temporal gyrus (yellow).

Table 1 Regions showing significant difference between AD and CN

	RESHARP				RESHARP with BSC			
	Without VR		With VR		Without VR		With VR	
	AD	CN	AD	CN	AD	CN	AD	CN
Precentral gyrus	8.1 ± 2.9**	6.5 ± 2.0**	7.5 ± 2.8**	5.9 ± 2.0**	7.1 ± 2.0**	5.8 ± 2.0**	6.4 ± 1.9**	4.8 ± 2.8**
Superior medial frontal gyrus	7.6 ± 3.0	6.5 ± 2.9	7.3 ± 3.1	6.2 ± 2.9	5.7 ± 2.6*	4.2 ± 3.0*	5.3 ± 2.7*	3.6 ± 3.3*
Hippocampus	–4.6 ± 3.5	–5.9 ± 3.5	–6.6 ± 3.7*	–8.4 ± 3.5*	–3.0 ± 3.8	–3.3 ± 6.2	–5.0 ± 4.1	–5.8 ± 6.1
Superior parietal gyrus	2.5 ± 3.1	1.8 ± 2.8	2.0 ± 3.1	1.3 ± 2.9	0.4 ± 2.3	–0.1 ± 2.1	–0.8 ± 2.6*	–2.0 ± 2.3*
Inferior temporal gyrus	–1.3 ± 1.8	–1.6 ± 1.8	–2.4 ± 2.0	–2.7 ± 1.9	–0.7 ± 1.4	–1.3 ± 1.5	–3.4 ± 1.5**	–4.4 ± 1.6**

Each data is presented as means ±. SD (ppb). *: $P < 0.05$. **: $P < 0.01$. AD, Alzheimer's disease; BSC, Brain surface correction; CN, Cognitive normal; RESHARP, Regularization enabled sophisticated harmonic artifact reduction for phase data; VR, Vein removal.

and VR). This can be associated with the variations in cortical susceptibility values among the subjects caused by streaking and other types of artifacts. For the mean QSM values in the parahippocampal gyrus and inferior temporal gyrus, the SDs were slightly high. The reason for this is probably due to susceptibility artifact from the skull base (for the hippocampus) and phase shift artifact from the ventricles. In addition to the suppression of artifacts, further studies are required to directly compare the results of QSM with those of neuropathology or PET studies.

Previous studies using QSM revealed a significantly higher susceptibility in the putamen of AD patients compared to the CN subjects.[7] However, a regional study did not

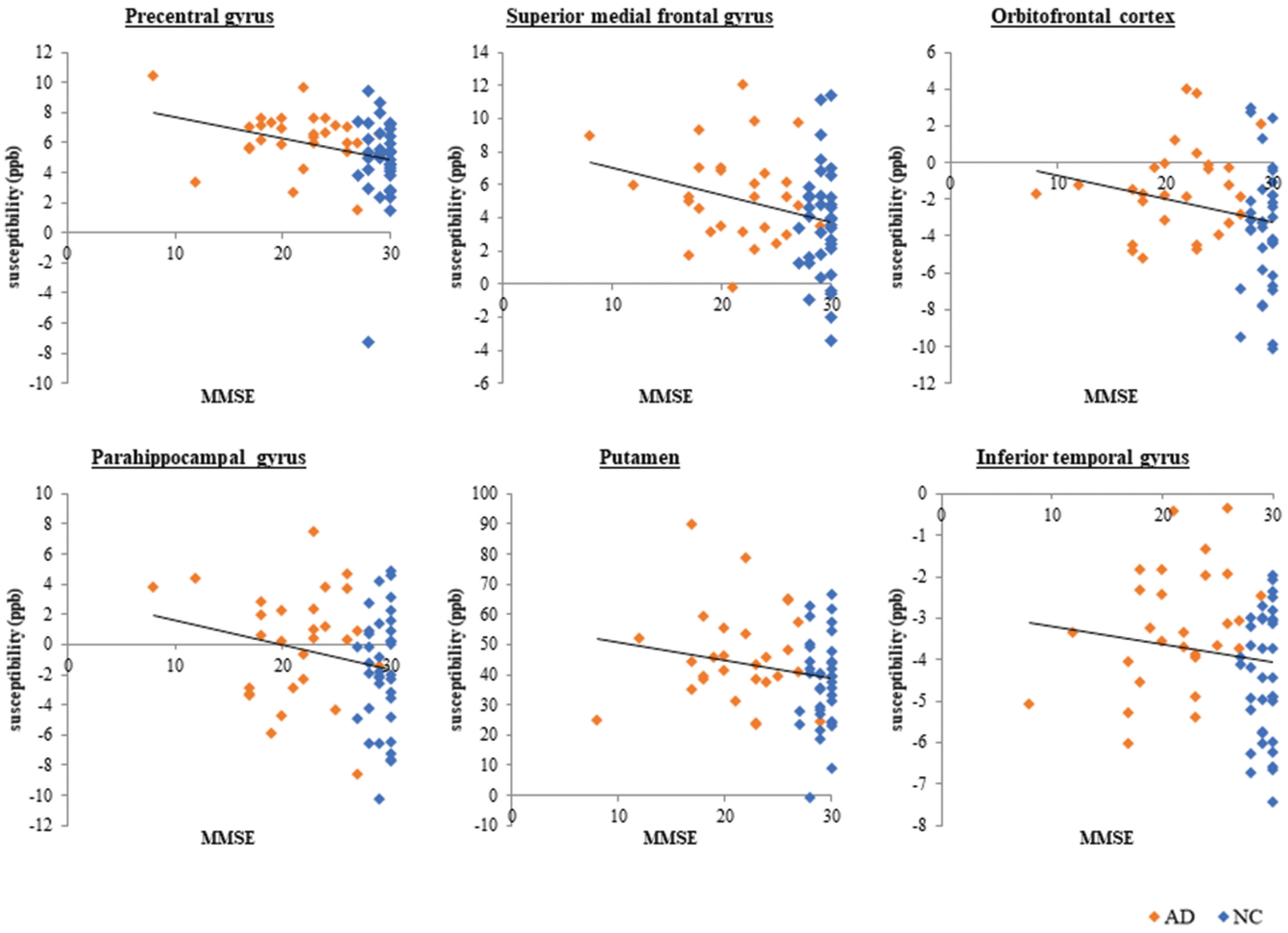

Fig. 3 Scatter plots between MMSE scores and the susceptibility values. MMSE scores had a significant correlation with the susceptibility values in the precentral gyrus and superior medial frontal gyrus. In contrast, we could not find a significant correlation in the orbitofrontal cortex, parahippocampal gyrus, putamen, and inferior temporal gyrus.

Table 2 Regions showing significant correlation between MMSE scores and the susceptibility values

	Regression equation	R^2	*P* value
Precentral gyrus	y = –0.14x + 9.12	0.08	0.02*
Superior medial frontal gyrus	y = –0.16x + 8.66	0.07	0.04*
Orbitofrontal cortex	y = –0.13x + 0.54	0.04	0.10
Parahippocampal gyrus	y = –0.16x + 3.22	0.05	0.09
Putamen	y = –0.60x + 56.51	0.04	0.13
Inferior temporal gyrus	y = –0.04x – 2.74	0.02	0.26

*: $P < 0.05$.

reveal any changes in the gray matter. The caudate nucleus and putamen showed similarity in increased susceptibility in another study.[22] Failure to select the gray matter as the ROI can be attributed to manual segmentation of the ROI structures. As mentioned above, several reports showed higher susceptibility in the basal ganglia in AD patients. Nonetheless, these studies did not focus on susceptibility in the cerebral cortex. This can be attributed to the difficulty in conducting QSM analysis on the surface of the brain, resulting in the exclusion of the surface areas.

According to Kim et al., QSM better differentiated AD from CN in regions, such as the hippocampus, precuneus, and allocortex (Brodmann area 4).[23] Increased susceptibility in the hippocampus and precuneus is compatible with AD pathology. Moreover, van Bergen et al. reported on the significant relationships between susceptibility and 18F-flutemetamol-standardized uptake value ratio (SUVR) in the frontal and temporal cortex.[8] Ayton et al. reported on the association between neocortical amyloid-β-SUVR and QSM values in the cortex of the frontal lobe, temporal lobe, and occipital lobe.[24] Despite the differences in the QSM calculation methods, the previous findings are consistent with our results. The latter focused on capturing the pathological changes in the cerebral cortex. Few studies have examined the susceptibilities in more segmented cortexes, similar to that in our study. With the increasing demand for visualizing pathological changes in the cerebral cortex, an accurate calculation of the susceptibility on the brain surface is warranted.

We removed cerebral veins by voxel with VR to exclude the influence of Oxygen Extraction Fraction (OEF). OEF is calculated from the susceptibility of deoxy-hemoglobin in thickened cortical veins by voxel. Deoxy-hemoglobin in reticular veins has little effect on the susceptibility in brain parenchyma because the ratio of vascular bed by sub-voxels is about 5%.[25,26] Actually, more regions of the cerebral cortex showed significantly higher susceptibility with VR. The venous voxels have higher susceptibility values because of deoxy-hemoglobin. Thus, without VR, the ROI measurements of the cerebral cortex may be inaccurate. In addition, AD patients may have a lower energy consumption,[27,28] thus reducing deoxy-hemoglobin in the veins. Therefore, the cortical ROI may show lower susceptibility, which counteracts an increase in the iron concentration. Therefore, the difference in susceptibility between AD patients and the CN subjects is likely to be smaller.

A previous study has reported a significant correlation between MMSE scores and the susceptibility values in the left caudate nucleus.[22] Although we observed a meaningful correlation between MMSE scores and the susceptibility values in the precentral gyrus and superior medial frontal gyrus, there was no strong correlation. In addition, we did not observe any substantial increase in susceptibility in the caudate nucleus. Further study is required to examine the correlation with more number of patients and a longer follow-up period.

Our study had some limitations. First, we chose an age-matched study; thus, the number of patients was relatively small. Second, we excluded the patients with microbleeds and calcification of the falx, which are common findings in elderly subjects. Third, we did not apply the multiple comparison correction, as this study aimed to compare the efficacy of BSC and VR. Fourth, we excluded cortical veins that are visible on QSM images. However, deoxy-Hb in the capillary vein within the parenchymal voxel may affect the cortical susceptibility values. We assumed that the effect was small, but it could not be excluded. Fifth, estimated susceptibilities in the brain surface depend on the reconstruction parameters of BSC. Therefore, in the present study, the optimized parameters were used to minimize calculation errors.[16] Sixth, we could not conduct a direct comparison of AD pathology. Further studies are required to compare our method of QSM and neuropathology, or at least other biomarkers, such as PET and cerebrospinal fluid (CSF). Seventh, we did not analyze the susceptibility in patients with mild cognitive impairment (MCI). Considering the gradual susceptibility changes expected in CN, MCI, and AD, evaluations including MCI are needed for the early diagnosis of the latter. In addition, further studies on other types of dementia, such as dementia with Lewy bodies and frontotemporal lobar degeneration, are of interest for determining the potential applications of QSM.

Conclusion

The newly developed method of QSM analysis for BSC and VR revealed more regions with significantly higher susceptibilities in AD patients. This preliminary study highlights the efficacy of this method in facilitating the diagnosis of AD and other neurodegenerative diseases.

Acknowledgments

We would like to thank Editage (www.editage.com) for English language editing.

Funding

Grant Support: This research was supported by AMED under Grant Number JP18he1402002.

Conflicts of Interest

Kohsuke Kudo (corresponding author) receives research funding from FUJIFILM Healthcare Corporation, and Ryota Sato, Yasuo Kawata, Toru Shirai, Hisaaki Ochi, and Yoshitaka Bito are employees of FUJIFILM Healthcare Corporation. The other authors declare that they have no conflicts of interest.

References

1. Jahn H. Memory loss in Alzheimer's disease. Dialogues Clin Neurosci 2013; 15:445–454.
2. Wilson RS, Segawa E, Boyle PA, Anagnos SE, Hizel LP, Bennett DA. The natural history of cognitive decline in Alzheimer's disease. Psychol Aging 2012; 27:1008–1017.
3. Rolston RK, Perry G, Zhu X, et al. Iron: A pathological mediator of Alzheimer disease? Agro Food Ind Hi-Tech 2009; 19:33–36.
4. Blennow K, Mattsson N, Scholl M, Hansson O, Zetterberg H. Amyloid biomarkers in Alzheimer's disease. Trends Pharmacol Sci 2015; 36:297–309.

5. Johnson KA, Sperling RA, Gidicsin CM, et al. Florbetapir (F18-AV-45) PET to assess amyloid burden in Alzheimer's disease dementia, mild cognitive impairment, and normal aging. Alzheimers Dement 2013; 9(Suppl):S72–S83.
6. Matsuda H. MRI morphometry in Alzheimer's disease. Ageing Res Rev 2016; 30:17–24.
7. Acosta-Cabronero J, Williams GB, Cardenas-Blanco A, Arnold RJ, Lupson V, Nestor PJ. In vivo quantitative susceptibility mapping (QSM) in Alzheimer's disease. PLoS One 2013; 8:e81093.
8. van Bergen JMG, Li X, Quevenco FC, et al. Simultaneous quantitative susceptibility mapping and Flutemetamol-PET suggests local correlation of iron and beta-amyloid as an indicator of cognitive performance at high age. Neuroimage 2018; 174:308–316.
9. Lovell MA, Robertson JD, Teesdale WJ, Campbell JL, Markesbery WR. Copper, iron and zinc in Alzheimer's disease senile plaques. J Neurol Sci 1998; 158:47–52.
10. Smith MA, Wehr K, Harris PLR, Siedlak SL, Connor JR, Perry G. Abnormal localization of iron regulatory protein in Alzheimer's disease. Brain Res 1998; 788:232–236.
11. Dixon SJ, Lemberg KM, Lamprecht MR, et al. Ferroptosis: an iron-dependent form of nonapoptotic cell death. Cell 2012; 149:1060–1072.
12. Ashraf A, Jeandriens J, Parkes HG, So PW. Iron dyshomeostasis, lipid peroxidation and perturbed expression of cystine/glutamate antiporter in Alzheimer's disease: Evidence of ferroptosis. Redox Biol 2020; 32:101494.
13. Tariq SH, Tumosa N, Chibnall JT, Perry MH 3rd, Morley JE. Comparison of the Saint Louis University mental status examination and the mini-mental state examination for detecting dementia and mild neurocognitive disorder—a pilot study. Am J Geriatr Psychiatry 2006; 14:900–910.
14. Nasreddine ZS, Phillips NA, Bédirian V, et al. The Montreal Cognitive Assessment, MoCA: a brief screening tool for mild cognitive impairment. J Am Geriatr Soc 2005; 53:695–699.
15. Sun H, Wilman AH. Background field removal using spherical mean value filtering and Tikhonov regularization. Magn Reson Med 2014; 71:1151–1157.
16. Shirai T, Sato R, Murase T, Bito Y, Ochi H. Whole brain background field removal using spherical mean value filtering and local polynomial approximation for quantitative susceptibility mapping. Proceedings of the 26th Annual Meeting of ISMRM, Paris, 2018; 4990.
17. Shirai T, Sato R, Taniguchi Y, Murase T, Bito Y, Ochi H. Quantitative susceptibility mapping using adaptive edge-preserving filtering. Proceedings of the 23rd Annual Meeting of ISMRM, Toronto, 2015; 3319.
18. Goto M, Abe O, Aoki S, et al. Diffeomorphic anatomical registration through exponentiated lie algebra provides reduced effect of scanner for cortex volumetry with atlas-based method in healthy subjects. Neuroradiology 2013; 55:869–875.
19. Tzourio-Mazoyer N, Landeau B, Papathanassiou D, et al. Automated anatomical labeling of activations in SPM using a macroscopic anatomical parcellation of the MNI MRI single-subject brain. Neuroimage 2002; 15:273–289.
20. Rolls ET, Joliot M, Tzourio-Mazoyer N. Implementation of a new parcellation of the orbitofrontal cortex in the automated anatomical labeling atlas. Neuroimage 2015; 122:1–5.
21. Rowe CC, Ng S, Ackermann U, et al. Imaging β-amyloid burden in aging and dementia. Neurology 2007; 68:1718–1725.
22. Du L, Zhao Z, Cui A, et al. increased iron deposition on brain quantitative susceptibility mapping correlates with decreased cognitive function in Alzheimer's disease. ACS Chem Neurosci 2018; 9:1849–1857.
23. Kim HG, Park S, Rhee HY, et al. Quantitative susceptibility mapping to evaluate the early stage of Alzheimer's disease. Neuroimage Clin 2017; 16:429–438.
24. Ayton S, Fazlollahi A, Bourgeat P, et al. Cerebral quantitative susceptibility mapping predicts amyloid-beta-related cognitive decline. Brain 2017; 140:2112–2119.
25. Kudo K, Liu T, Murakami T, et al. Oxygen extraction fraction measurement using quantitative susceptibility mapping: Comparison with positron emission tomography. J Cereb Blood Flow Metab 2016; 36:1424–1433.
26. Uwano I, Kudo K, Sato R, et al. Noninvasive assessment of oxygen extraction fraction in chronic ischemia using quantitative susceptibility mapping at 7 tesla. Stroke 2017; 48:2136–2141.
27. Yin F, Sancheti H, Patil I, Cadenas E. Energy metabolism and inflammation in brain aging and Alzheimer's disease. Free Radic Biol Med 2016; 100:108–122.
28. Blonz ER. Alzheimer's disease as the product of a progressive energy deficiency syndrome in the central nervous system: the neuroenergetic hypothesis. J Alzheimers Dis 2017; 60:1223–1229.